INTERNATIONAL JOURNAL OF INTEGRATED ENGINEERING
ISSN: 2229-838X e-ISSN: 2600-7916

IJIE

Vol. 16 No. 5 (2024) 489-502
https://publisher.uthm.edu.my/ojs/index.php/ijie

Effectiveness of Porous Durian Shell-based Activated Carbon for Methylene Blue Adsorption

R. Mohamat[1,2], A. B. Suriani[1,2]*, A. Mohamed[1], A. Kamari[1], Muqoyyanah[1,3], M. H. D. Othman[4], M. H. Mamat[5], M. K. Ahmad[6], M. N. Azlan[2], N. Hashim[1], M. A. Mohamed[7], M. D. Birowosuto[8], T. Soga[9], H. H. Kusuma[10], B. Astuti[11] and K. Ali[12]

1 *Nanotechnology Research Centre, Faculty of Science and Mathematics, Universiti Pendidikan Sultan Idris, 35900 Tanjung Malim, Perak, MALAYSIA*
2 *Department of Physics, Faculty of Science and Mathematics, Universiti Pendidikan Sultan Idris, 35900 Tanjung Malim, Perak, MALAYSIA*
3 *Research Center for Nanotechnology System, National Research and Innovation Agency (BRIN), South Tangerang, Banten, 15314, INDONESIA*
4 *Advanced Membrane Technology Research Centre (AMTEC), Faculty of Chemical and Energy Engineering (FCEE), Universiti Teknologi Malaysia, 81310 Skudai, Johor, MALAYSIA*
5 *NANO-ElecTronic Centre (NET), School of Electrical Engineering, College of Engineering, Universiti Teknologi MARA, 40450 Shah Alam, Selangor, MALAYSIA*
6 *Microelectronic and Nanotechnology–Shamsuddin Research Centre (MiNT-SRC), Faculty of Electrical and Electronic Engineering, Universiti Tun Hussein Onn Malaysia, 86400 Parit Raja, Batu Pahat, Johor, MALAYSIA*
7 *Institute of Microengineering and Nanoelectronics (IMEN), Universiti Kebangsaan Malaysia, UKM Bangi, Selangor 43600, MALAYSIA*
8 *Łukasiewicz Research Network-PORT Polish Center for Technology Development, Stabłowicka 147, Wrocław 54-066, POLAND*
9 *Department of Electrical and Mechanical Engineering, Nagoya Institute of Technology, Gokiso-cho, Showa-ku, Nagoya, 466-8555, JAPAN*
10 *Department of Physics, Faculty of Sciences and Technology, Universitas Islam Negeri Walisongo Semarang, Central Jawa, INDONESIA*
11 *Study Program of Physics, Faculty of Mathematics and Natural Sciences, Universitas Negeri Semarang, Sekaran, Gunungpati, Central Java, Semarang 50229, INDONESIA*
12 *Nano-optoelectronics Research Laboratory, Department of Physics, University of Agriculture Faisalabad, 38040 Faisalabad, PAKISTAN*

*Corresponding Author: suriani@fsmt.upsi.edu.my
DOI: https://doi.org/10.30880/ijie.2024.16.05.037

Article Info

Received: 21 January 2024
Accepted: 27 May 2024
Available online: 29 August 2024

Keywords

Activated carbon, durian shell, sulphuric acid, adsorption, dye

Abstract

In this study, durian shell-based activated carbon (DAC) was produced via chemical activation method by utilising durian shell and sulphuric acid (H_2SO_4) as the starting material and activating agent, respectively. The incorporation of H_2SO_4 in the DAC production process resulted an improvement in the surface properties and adsorption capacity of the produced DAC adsorbent. Field emission scanning electron microscopy analysis further showed that the produced DAC possessed a porous structure which was beneficial for dye adsorption application. Under operating conditions of 500°C and 3 hours carbonisation temperature and time, the Brunauer–Emmett–Teller (BET) surface area, total pore volume and BET average pore diameter were measured to be 242.03 m^2/g, 0.028 cm^3/g and 2.28 nm, respectively. The adsorption performance of the produced DAC was then investigated using methylene blue (MB) as the model adsorbate. The optimum MB dye

removal and adsorption capacity were found to be 92.05% and 0.767 mg/g, respectively, with 0.6 g of DAC dosage, 10 ppm of initial MB dye concentration and 15 min of contact time.

1. Introduction

Dyes are widely used in the dyeing, textiles, plastics, leather, cosmetics and food industries. The discharge of colouring contaminants in water causes environmental problems. Dyes are carcinogenic and hazardous to aquatic living organisms, and their stable aromatic molecular structure make this problem more extreme because large amounts of dyes are being discharged day by day [1]–[3]. Various methods have been introduced to degrade and remove these dyes, including chemical precipitation or oxidation, coagulation/flocculation, electrochemical processes, membrane separation, photocatalysis and adsorption [2], [4]–[12]. Among them, adsorption process is considered as a versatile and effective dye removal method due to its several advantages, such as low-cost, high efficiency, eco-friendliness and ease of operation [2], [13], [14]. In adsorption method, type of adsorbent plays a crucial role in adsorption performance as well as removal percentage. Several adsorbents that have been used for adsorption process include activated carbon (AC) [6], [14], metal oxide [15], biosorbents [16] and zeolites [17]. Among these adsorbents, AC becomes the most promising material thus widely used due to its convenient properties, such as large surface area and high adsorption capacity with microporous morphological structure [18]–[20].

Commercial AC is uneconomical and commonly fabricated from expensive precursors and non-renewable materials such as coal and lignite, thereby hindering its usage as an adsorbent [21]. With regard to the aforementioned limitation, the low-cost and renewable carbonaceous materials such as peat, crops, agricultural and organic waste [22] with an equivalent adsorption capacity as commercial AC has been widely developed [19]. Moreover, it is also a fact that a large number of agricultural wastes are being discarded every year, thereby causing waste management problems. This condition has led to the production of AC by utilising agricultural waste variety as a precursor, including green coconut shell and bamboo [4], pumpkin peels [19], palm kernel shell [23], banana stem [24], lapsi seed stone [25], papaya peel [26], Ficus carica bast [27] and durian shell (DS) [28]–[30].

About 209,343 metric tons of durian fruit were produced in Malaysia in 2017 and estimated to increase in the following years [31]. The durian fruit consists of 40% flesh and 60% DS waste. DS has no economic value thus usually burned without considering the surrounding environment. Its abundance and availability then can be used as a good raw material source for AC production since this material possesses high carbon and low ash content [28]. In addition, the AC conversion using agricultural waste would enhance the value of agricultural commodities and at the same time decrease the waste disposal cost and provide a potential alternative to economic AC. Basically, AC based on agricultural waste can be produced via two methods: physical and chemical activation [20], [23], [32].

Physical activation involves the carbonisation of the precursors in an inert gas before activation process by using oxidising agents such as steam and carbon dioxide. Meanwhile, chemical activation is a single-step method that includes the simultaneous process of carbonisation and activation. In chemical activation, the impregnation process of the precursor can be performed with a chemical activator such as sulphuric acid (H_2SO_4) [13], [27], zinc chloride ($ZnCl_2$) [32], potassium hydroxide (KOH) [14], [26] and phosphoric acid (H_3PO_4) [23], [24]. A comparison between the methods shows that chemical activation offers several advantages, including low energy usage, low operating temperature and high carbon yields [20]. Furthermore, pore structure development can be modified by changing parameters such as temperature during the carbonisation process, impregnation ratio and type of activating agent [32].

The dye removal performance of AC is strongly depended on its adsorption capacity (qe) and surface area. Three factors that determine the qe value are type of activator agent, pyrolysis temperature and activation time [21]. Among several activator agents, H_2SO_4 is a super oxidising agent that is widely used for the preparation of carbonaceous adsorbents [33]. Sahira et al. [25] successfully prepared AC from lapsi seed stone that was initially impregnated with H_2SO_4. Higher qe (156 mg/g) was achieved as compared with the utilisation of ferric chloride (108 mg/g) and magnesium chloride (135 mg/g) due to a well-developed mesoporosity of H_2SO_4 [25]. Recently, Jawad et al. [33] showed that watermelon peels can be successfully converted into AC by utilising H_2SO_4 and presented excellent performance in methylene blue (MB) removal from aqueous solution. They also reported that the dye removal percentage reached 99% with a maximum qe value of 200 mg/g [33].

AC with a different surface area can also be synthesised from the same precursor with different carbonisation time and temperature. Nicholas et al. [23] showed that a carbonisation temperature of 500°C produced the highest surface area. However, a lower surface area was observed when the carbonisation temperature was increased up to 700°C [23]. This result was in a good agreement with the data presented by Srinivasakannan et al. [34]. They found that the optimised carbonisation temperature was around 400–500°C depending on the impregnation ratio and carbonisation time. They also found that the optimum carbonisation process time was around 1–3 hours. However, lower AC product and higher surface area were achieved by increasing the carbonisation time [34].

Int. Journal of Integrated Engineering Vol. 16 No. 5 (2024) p. 489-502

A series of experiments have been successfully conducted to study the performance of durian-based AC. Ismail et al. [35] produced AC from durian seed by utilising H_3PO_4 as a chemical activator. They impregnated 10–20 g of durian seed that has a particle size of around 500–710 µm with H_3PO_4. The mixture was then subjected to low-temperature treatment (150°C) in a muffle furnace under nitrogen gas flow for 2 hours before the final treatment of 600–900°C for 4 hours with different heating rates. The obtained Brunauer–Emmett–Teller (BET) surface area was 2123 m^2/g with a total surface area of 2147 m^2/g [35]. Meanwhile, Foo and Hameed [36] prepared AC from DS through physical activation assisted by NaOH. Carbonisation process was performed by loading 500 g of dried DS precursor into a vertical furnace at a temperature of 700°C under nitrogen gas flow. The BET surface area of DS-based AC (DAC) was 1475.46 m^2/g with a total pore volume of 0.841 cm^3/g. In addition, the qe value was around 410.85 mg/g [36].

In 2015, Mahmood et al. [29] produced durian-based AC by carbonising 25 g of DS at temperature of 350°C for 1 hour. Then, the produced char was activated with KOH and H_3PO_4. The impregnation process was performed by stirring the sample for 5 hours at room temperature until a slurry solution was observed. Then, the sample was dried in an oven for 24 hours before the second carbonisation was performed at 500°C under the same condition as the previous carbonisation process. The results showed that the H_3PO_4-activated DS has a higher surface area (257.50 m^2/g) compared with KOH-activated DS (13.10 m^2/g) [29].

Most studies have reported the production of DS by utilising various activator agents with different carbonisation temperature and time [28], [29], [35], [37]. However, insufficient information was found on obtaining DAC by utilising H_2SO_4 as chemical activator. Therefore, this work is the first attempt to use H_2SO_4 as a chemical activator to produce high-quality AC from DS for MB dye removal in wastewater because the previous report focused more on using KOH and H_3PO_4 [29], [35], [37]. Therefore, in this study, DS as an agricultural waste is used as a precursor to produce AC by utilising H_2SO_4 as the activator agent via chemical activation. Furthermore, the produced DAC was used to investigate its performance in the adsorption process for MB removal.

2. Chemicals and Materials

2.1 Materials

DS as a starting material was obtained from the market around Tanjong Malim, Perak, Malaysia. H_2SO_4 (95%–97%, Merck) was utilised as an activating agent. Meanwhile, MB dye (Sigma-Aldrich) was used for the adsorption studies.

2.2 Preparation of AC

Prior to the process, fresh DS was washed with deionised water to remove other impurities or dusk. As an initial step, the fresh DS was cut into small pieces before it underwent the dehydration process. This process was performed to reduce the moisture content of DS since fresh DS has a high-water content. The DS dehydration process was carried out twice: (1) drying under the sun for 3 days then (2) drying in the oven for 24 hours at 80°C. The dried DS was then ground by using a blender. Next, 60 g of ground DS was treated with 30 mL of H_2SO_4 at room temperature for 24 hours. The sample was then annealed for 3 hours at 500°C to perform the carbonisation process. Next, the produced DAC was crushed into powder form by using a mortar.

3. Characterisation Methods

3.1 Activated Carbon Characterisation

The morphology of DAC was characterised using field emission scanning electron microscopy (FESEM) (Hitachi SU8020). The specific surface area and total pore volume of DAC were determined by using a surface area and porosity analyser (Micromeretics ASAP 2020). The BET surface area was determined by calculating the amount of adsorbate gas corresponding to a monomolecular layer on the surface of the material. The total pore volume was then determined by using Barrett–Joyner–Halenda method. Meanwhile, micro-Raman spectroscopy (Renishaw InVia microRaman System) was used to study the structural properties of the produced DAC. The treated dye solution after the adsorption process was further characterised using UV-Vis spectroscopy (Cary 60 UV-Vis, Agilent Technologies).

3.2 Adsorption Performance

MB adsorption was conducted to evaluate the performance of the produced DAC. The adsorption test was carried out at room temperature with different parameters. The MB solution volume (50 mL) and stirring speed were kept constant during the test. To determine the optimum initial dosage of adsorbent, 0.2, 0.6, 1.0, 1.4, 1.8 and 2.2

g of DAC were added to the MB solution at an initial concentration of 10 ppm. Then, the solution was stirred at a constant speed for 15 min.

Next, to study the optimum initial MB concentration, the previous optimum initial dosage of adsorbent was added to different initial MB concentrations (2.5, 5, 7.5, 10 and 25 ppm). The solution was stirred for 15 min at a constant speed. Next, the obtained dosage of adsorbent and initial concentration was used to study the optimum contact time. The solution was then stirred for 5, 10, 15, 20, 25 and 30 min.

The removal percentage and the adsorption capacities of DAC were determined using the following equations.

$$R(\%) = \left[1 - \frac{C_f}{C_o} \times 100\%\right] \quad (1)$$

$$q_e = (C_o - C_f) \times \frac{V}{m} \quad (2)$$

where R is the removal rate of MB; C_o (mg/L) and C_f (mg/L) is the initial and final concentration of the MB solution, respectively; V (L) is the volume of the solution, and m (g) is the dosage of the adsorbent.

4. Results and Discussion

4.1 Morphological Properties

FESEM images of the produced DAC are presented in Fig. 1. The surface morphology of DAC is smooth with no agglomeration of the granular structure, as shown in Fig. 1(a). Higher magnification shows that the produced DAC has a porous structure (Fig. 1(b)) and several visible holes (see insert picture in Fig. 1(c)) distributed on the entire DAC surface. The high porosity of DAC sample is believed to provide a larger surface area, as stated in several works [20], [38]. In addition, the DAC sample possessed pores surrounded by an interconnected irregular shape, as shown in Fig. 1(d). This condition might be due to the activation condition, including the use of H_2SO_4 as an activator agent, which influenced the porosity characteristics of DAC samples, such as the pore size distribution and shapes of the pores [33]. The obtained morphology is in a good agreement with Mahmood et al. [29] and Ukkakimapan et al. [5] where porous structure (sponge-like structure) with the cavities was well pronounced after the DAC was treated with chemical activator.

The development of the pores can be related to the breakdown of some DS material due to thermal expansion during the activation process [33], [38]. During the chemical activation process, H_2SO_4 as a chemical activator deeply penetrated the carbon structure, which then developed tiny pores [33]. The activator agent was believed to be responsible for the porosity development of the starting material by widening the existing pores and creating new pores. In addition, full development of porosity was caused by the prolonged heat treatment (3 hours) during the activation process [39]. The developed pores are considered to provide an advantage in the adsorption process.

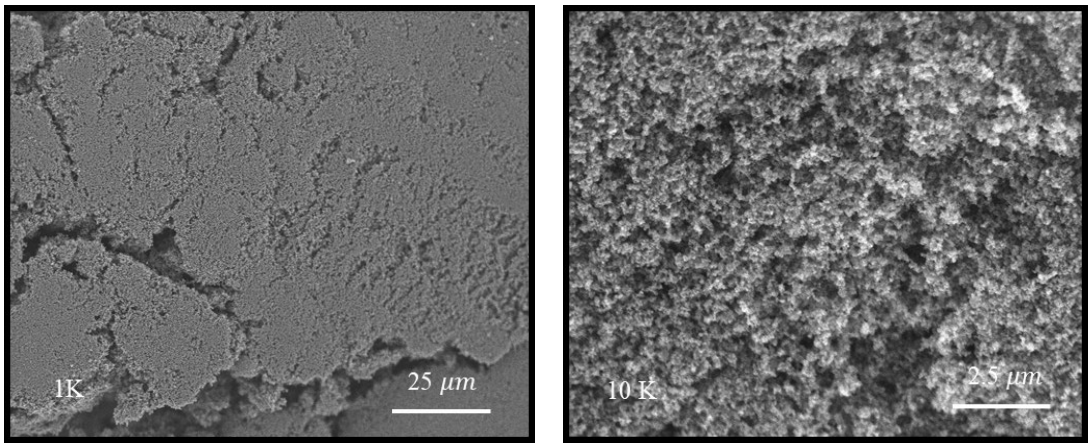

(a) **(b)**

Int. Journal of Integrated Engineering Vol. 16 No. 5 (2024) p. 489-502

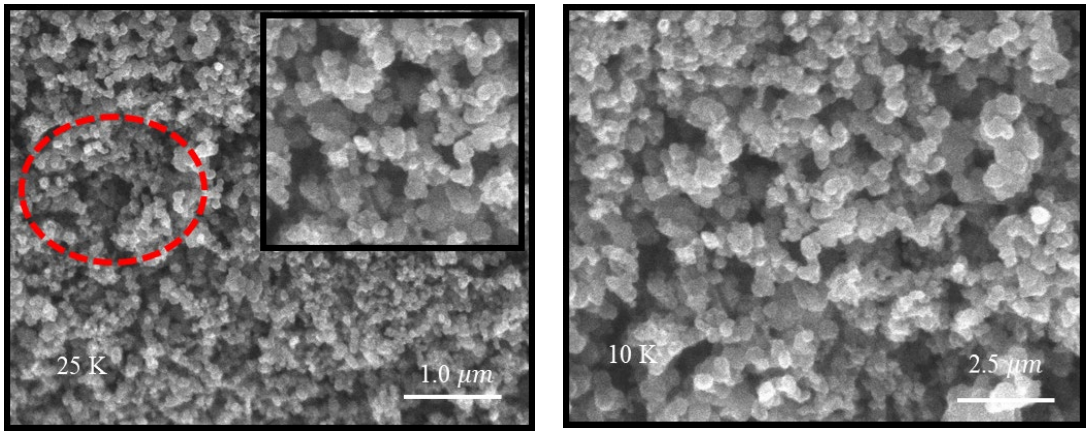

Fig. 1 *FESEM images of; (a) Overall surface morphology; (b) Porous structure; (c) Visible hole; and (d) Pore shapes of the produced DAC*

4.2 Micro-Raman Spectroscopy

The DAC graphitic existence was then confirmed by micro-Raman spectroscopy. Fig. 2 shows that the DAC sample possesses two peaks at 1402.2 and 1585.8 cm^{-1}, which correspond to the D- and G-band of the typical spectrum observed for carbon materials, respectively. The D-band in the DAC sample indicates the disordered graphite structure that refers to the existence of graphitic characteristics. Meanwhile, G-band indicates the sp^2 carbon network which confirmed the graphitic presence in the sample [23]. Furthermore, the ratio between D- and G-band peak intensity (I_D/I_G) ratio of the fabricated DAC can be used to investigate the defect or graphitic order. On the basis of calculations, the I_D/I_G ratio presented by DAC sample was 0.91, indicated a higher graphitic content over the defect components [23], [40] and proved lower damage to the carbon structure of DAC during the activation process.

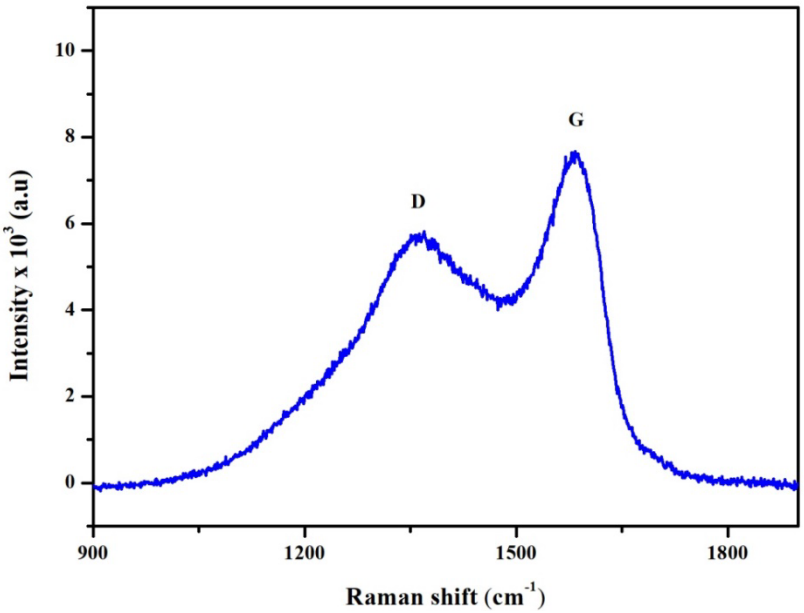

Fig. 2 *Micro-Raman spectra of the produced DAC*

4.3 Surface Area Analysis

The BET surface area of H_2SO_4-treated DAC was found to be 242.03 m^2/g with 0.028 cm^3/g total pore volume. The total pore volume presented by DAC was related to the porosity development, which significantly affected the performance of AC during the adsorption process [29]. Moreover, the BET average pore diameter value (D_p) for H_2SO_4-treated DAC was 2.28 nm, which confirmed the presence of mesopore as internal pores. The correlation between internal pores and BET value was also confirmed by other report. H_3PO_4-treated DAC which possessed both of mesopores and macropores showed slightly higher BET surface area of 257.50 m^2/g compared to this study [29]. However, the BET surface area of this study was found to be much higher than that of KOH-treated

DAC (13.10 m^2/g) which only resulted micropores as internal pores [29]. This confirmed the effective and comparative H_2SO_4 to be used as activating agent compared to KOH and H_3PO_4, respectively. The BET surface area of DAC can further be increased by dehydrating the DS using H_2SO_4 and subsequently activating it by NaOH as chemical reagent. Recently, Ukkakimapan et al. [5] reported the highest DAC's BET surface area of 2578 m^2/g with the formation of meso-macro pores. They reported that the dehydration route is one of the factors that contributed to the higher BET surface area. This result can be adopted for further improvement of this study. However, the mesopores as internal pores obtained in this study was believed to enhance the DAC adsorption process because it is suitable for application in liquid-phase processes [41].

Apart from different activator agent, the lower BET surface area presented in this study as compared to other reports might be due to the different activation temperature and activation time. Based on the literature, as the activation temperature increased, the BET surface area also increased which might resulted the formation of new pores since the volatile matter was released [42]. This statement has been confirmed by Ismail et al. [35] and Ukkakimapan et al. [5] based on their results. The BET surface area comparison of Durian-based AC treated with different activator agent are presented in Table 1.

Table 1 *The BET surface area comparison of Durian-based AC treated with different activator agent*

Adsorbent	Preparation method	Activator agent	Impregnant ratio of durian to activator agent	Activation temperature (°C)	Activation time	BET surface area (m^2/g)	Total pore volume (cm^3/g)	Reference
Durian shell	Chemical activation	H_2SO_4	2	500	3 h	242.03	0.028	This study
Durian shell	Physical activation	CO_2	-	550	15 min	917	0.447	[30]
Durian shell	Chemical activation	H_2SO_4 (Dehydration agent) and NaOH (activator agent)	0.4	720	1 h	2578	1.27	[5]
Durian shell	Chemical activation	H_3PO_4	0.5	500	1 h	257.50	0.149	[29]
		KOH				13.10	0.022	
Durian seed	Chemical activation	H_3PO_4	2	600	4 h	2123	0.904	[35]
Durian shell	Chemical activation	KOH	0.5	~500	1 h	992	0.411	[37]

4.4 Dye Removal Performance

4.4.1 Effect of DAC Dosage

Determining the optimum DAC dosage for efficient MB removal is important to prevent excessive adsorbent usage. In this study, various DAC dosage in the range of 0.2 to 2.2 g were used with a constant MB concentration (10 ppm) and contact time (15 min) and the results are shown in Fig. 3 (pink graph). The relative MB removal percentage for 0.2 and 0.6 g DAC dosage increased rapidly from 81.53 to 92.05%, respectively. This result was believed due to the larger surface area of DAC when the dosage was increased thus offer more available vacant active sites during the adsorption process [19], [33]. However, the MB removal percentage was almost constant when the DAC dosage was increased over 0.6 g adsorbent mass.

As depicted in Fig. 3 (pink graph), the MB removal percentage of 1.0–2.2 g of DAC dosage was almost constant with the value of 92.47–92.63 % (Table 2). This result might be caused by the aggregate formation of adsorbent particles (DAC) during the adsorption process when the DAC dosage was increased. Higher DAC aggregation formation leads to the lower effective accessible adsorption area [27], [33]. This result was in a good agreement with the final concentration of treated water value, which decreased from 1.847 to 0.737 ppm (Table 2). These

Int. Journal of Integrated Engineering Vol. 16 No. 5 (2024) p. 489-502

results suggest that the optimum DAC dosage was 0.6 g by utilising 10 ppm of MB solution with 15 min contact time.

Further measurement shows that the adsorption capacity (q_e) of DAC rapidly decreased from 2.038 to 0.767 mg/g when the DAC dosage was increased from 0.2 to 0.6 g, respectively (see blue graph in Fig. 3). By increasing the DAC dosage from 1.0 to 1.8 g, lower q_e value of 0.462–0.258 mg/g was obtained (Table 2). Further utilisation of higher DAC dosage (2.2 g) then resulted slightly lower q_e value of 0.210 mg/g. These results confirmed that a lower DAC dosage had a higher adsorption rate per unit as the consequence of higher available MB molecules to be adsorb onto the DAC surface [19].

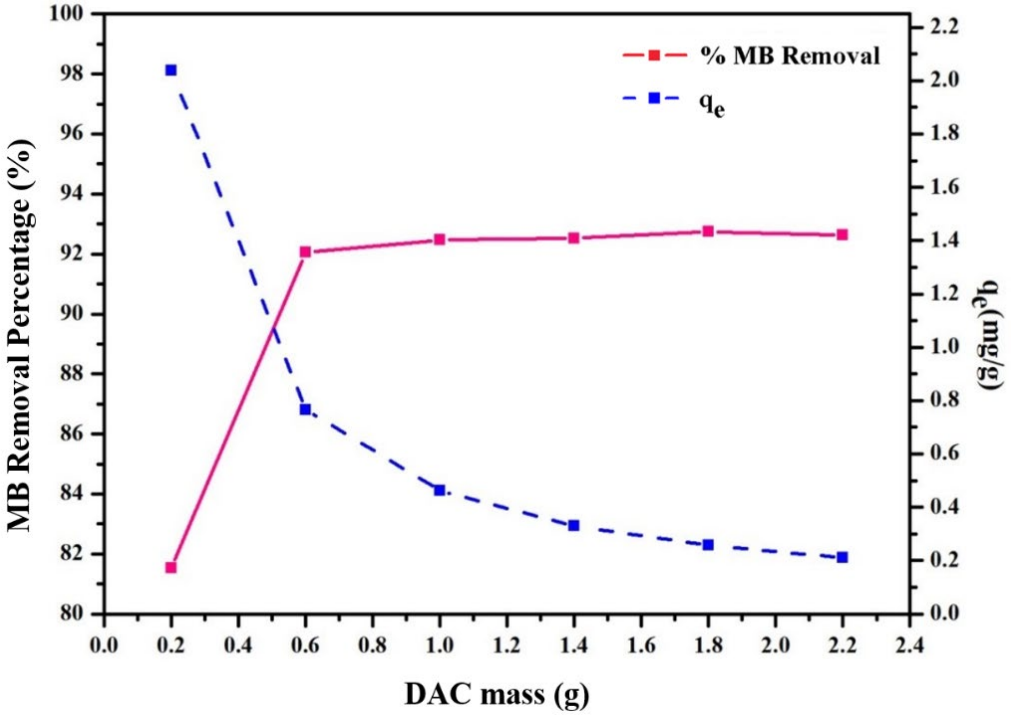

Fig. 3 *MB removal percentage and its adsorption capacity by utilising different DAC dosage measured with 10 ppm MB dye and 15 min contact time*

Table 2 *Adsorption performance of the produced DAC measured at different DAC dosages*

DAC dosage (g)	Final concentration (ppm)	MB removal percentage (%)	Adsorption capacity; q_e (mg/g)
0.2	1.847	81.53	2.038
0.6	0.795	92.05	0.767
1.0	0.753	92.47	0.462
1.4	0.747	92.53	0.330
1.8	0.725	92.75	0.258
2.2	0.737	92.63	0.210

4.4.2 Effect of Initial MB Dye Concentration

On the basis of previous measurement, the adsorption efficiency was further investigated by utilising different initial MB dye concentrations of 2.5, 5, 7.5, 10 and 25 ppm (50 mL) with 0.6 g of DAC dosage and 15 min of contact time. Fig. 4 (see pink graph) shows that the MB removal percentage increased significantly from 63.25 to 92.05% (0.919 ppm to 0.795 ppm of treated water final concentration) by utilising 2.5–10 ppm initial MB dye, respectively. However, the dye removal percentage decreased to 86.67% when the initial MB dye concentration was increases to 25 ppm with a higher final concentration of treated water of 3.332 ppm compared to other initial MB dye

concentrations. This result was believed due to the limitation of available active sites on the adsorbent surface when the initial concentration was increased up to 25 ppm [20]. On the basis of the results, the optimum initial MB dye concentration was 10 ppm by utilising 0.6 g DAC dosage and 15 min contact time.

Further measurement also showed that the q_e significantly increased from 0.132 to 1.805 mg/g with the increment of initial MB dye concentration (see blue graph in Fig. 4). Increasing the initial MB dye concentration resulted in a higher driving force that moved MB towards the adsorption sites [14], [36]**.** At a high initial MB dye concentration, more MB molecules are available to interact with DAC [6] thus resulted higher q_e value. The adsorption performance of the produced DAC measured at different initial MB dye concentrations are summarised in Table 3.

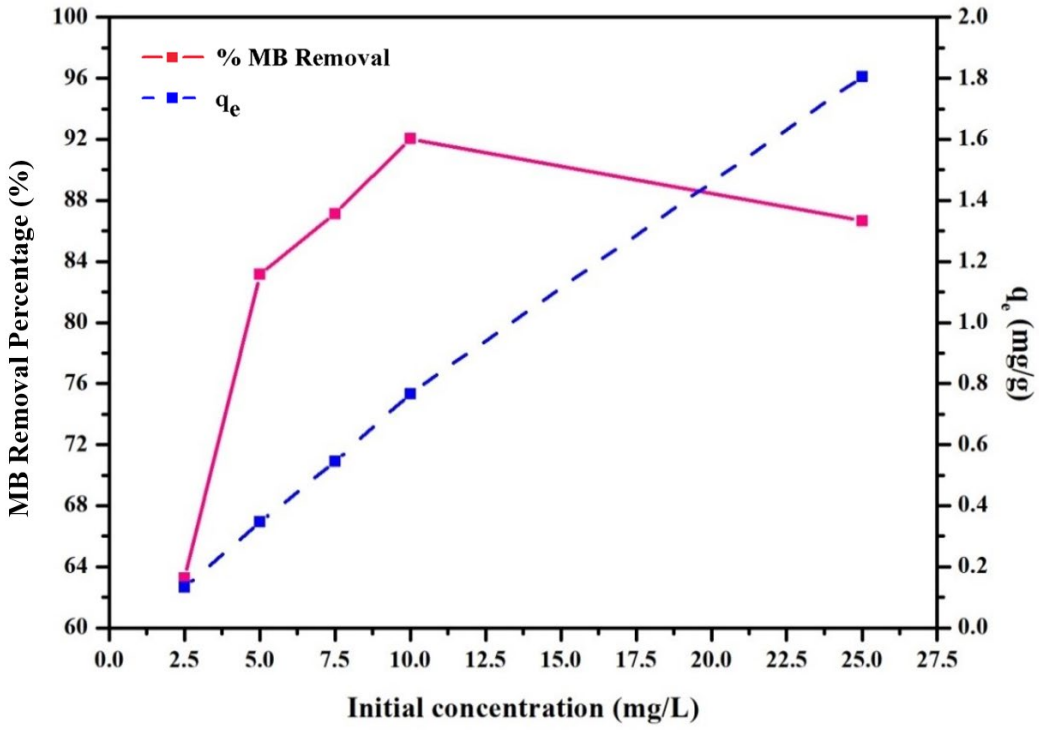

Fig. 4 *MB removal percentage and its adsorption capacity by utilising different initial MB concentration with 0.6 g DAC dosage and 15 min contact time*

Table 3 *Adsorption performance of the produced DAC measured at different initial MB dye concentrations*

Initial concentration (ppm)	Final concentration (ppm)	MB removal percentage (%)	Adsorption capacity, q_e (mg/g)
2.5	0.919	63.25	0.132
5	0.843	83.14	0.346
7.5	0.966	87.12	0.544
10	0.795	92.05	0.767
25	3.332	86.67	1.805

4.4.3 Effect of Contact Time

Contact time plays a crucial role in the adsorption process [43], [44]. Dye removal and the corresponding contact time were further studied by using a fixed amount of adsorbent dosage and initial MB concentration of 0.6 g and 10 ppm (50 mL of volume), respectively. Fig. 5 represents the MB removal percentage and its q_e value with respect to contact time. The summary of final concentration, MB removal percentage and DAC adsorption capacity are shown in Table 4. The MB removal percentage was observed to be slightly increased from 91.25 to 91.89% during the initial stage of 5–10 min and gradually increased to 92.05% (15 min) with final concentrations of 0.875, 0.811 and 0.795 ppm, respectively. This finding shows that a higher amount of adsorbed MB was observed by

Int. Journal of Integrated Engineering Vol. 16 No. 5 (2024) p. 489-502

performing longer contact time. The MB molecules have the tendency to diffuse into the porous structure of DAC and utilise the active site when longer contact time was performed [45]. However, a slower adsorption process was observed after 20 to 30 min of contact time, which resulted lower MB removal percentage of 91.79 and 88.58% (0.821 and 1.141 ppm of final concentration), respectively. This result might be caused by the lack of available active sites for dye adsorption when contact time was prolonged [36].

The calculated q_e value also showed a similar trend with MB removal percentage. The increment of q_e value from 0.760 to 0.766 mg/g was observed during the initial stage of adsorption process (5–10 min). By further increasing contact time of 15 min, optimum MB adsorption was obtained with an optimum q_e value of 0.767 mg/g (blue graph). This result was caused by faster adsorption process as the consequence of numerous and available vacant active sites by DAC during the starting point [6]. However, the q_e value of DAC decreased from 0.764 to 0.738 mg/g when contact time was increased from 20 to 30 min due to the lack of available active sites required for further uptake of MB molecules [46]. Based on these results, the optimum contact time for adsorption process of MB molecules onto the DAC surface was 15 min.

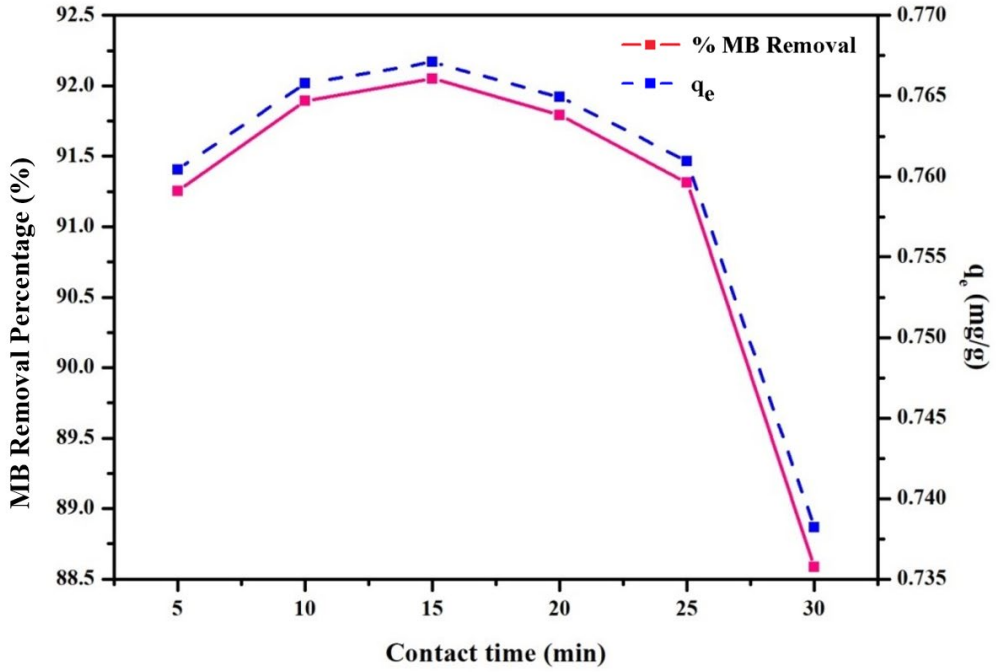

Fig. 5 *MB removal percentage and its adsorption capacity by utilising different contact time with 0.6 g DAC dosage and 10 ppm of initial MB dye concentration*

Table 4 *Adsorption performance of the produced DAC measured at different contact times*

Contact time (min)	Final concentration (ppm)	MB removal percentage (%)	Adsorption capacity, q_e (mg/g)
5	0.875	91.25	0.760
10	0.811	91.89	0.766
15	0.795	92.05	0.767
20	0.821	91.79	0.764
25	0.869	91.31	0.760
30	1.141	88.58	0.738

4.5 Mechanism of Adsorption

The pore size of DAC in this study is 2.28 nm in diameter (Table 1), while the depth, width and thickness of MB are 0.61, 1.43 and 0.4 nm, respectively [47]. Therefore, it is assumed that the MB dye was easily accessible within the DAC porous structure. The adsorption mechanism of DAC was assumed to involve the external and internal diffusion through four possibilities as shown in Fig. 6(a) [6], [48]. First, the adsorption process of MB dye

molecules from the bulk liquid phase into the solid phase (DAC) began when the MB molecules is brought in contact with DAC surface. Second, MB molecules migrated from the bulk solution to the external boundary layer of DAC surface [49]. Third, the MB molecules were transported from the DAC surface into the active site on the interior surfaces of the pores. Fourth, the MB molecule approached the DAC internal pores by intra-particle diffusion.

Concurrently, it is also believed that the MB molecules adsorption onto the DAC occurred due to the chemical link between the MB^+ ion (molecule being adsorbed) and the DAC (adsorbent) [49]. By definition, MB is cationic dyes with cationic properties originating from positively charged nitrogen (N) or sulphur (S) atoms [50]. Therefore, it was believed that the following mechanisms occurred; the electrostatic interaction (mechanism I), formation of hydrogen bonding (mechanism II), electron donor-acceptor (mechanism III) and π- π dispersion interaction (mechanism IV) as shown by Fig. 6(b). As being stated by Vargas et al. [51], the presence of surface functional groups plays a crucial role for q_e and MB dye removal mechanism. Therefore, mechanism (I) can be explained based on the electrostatic interaction between cationic N presented in MB and negatively charged site of carboxylate ion ($-COO^-$) on the DAC surface as shown in Fig. 6(b)(I).

Meanwhile, mechanism (II) proposed the hydrogen bonding which commonly occurs in most adsorption system. The presence of hydroxyl group on DAC surface had been confirmed through Fourier transform infrared by previous study conducted by Foo and Hameed [36]. The hydrogen bonding interaction can be formed between the surface hydrogens of the hydroxyl group on the DAC surface and N atom of MB (Fig. 6(b)(II)). The hydrogen bond existence between the –OH group of DAC and the –N groups of MB consequently support the MB removal process.

Mechanism (III) involved the electron donor-acceptor between the surface functional group (carbonyl oxygen) as an electron donor and the MB aromatic structure (electron acceptor) (Fig. 6(b)(III)). These interaction resulted in reducing the blue colour of MB into colourless leucomethylene [52]. In addition, the presence of higher surface area (as supported by BET surface area) and more active sites of DAC compared to other produced AC including KOH-treated DAC (13.10 m^2/g) and pumpkin peels-based AC (3.6 m^2/g) [19], [29] augmented the MB sorption through electron donor-acceptor interaction between DAC aromatic skeleton and MB cations. As a results, H_2SO_4-treated DAC presented better MB removal than the mentioned produced AC. From the reported literature, DAC possessed aromatic structure of graphene layers [49], [51], [53]. Since the MB also owns aromatic structure, therefore mechanism (IV) might be happened through π- π dispersion interaction between aromatic structure of MB and DAC (Fig. 6(b)(IV)). This leads to a speculation that DAC predominantly functionalised by other active sites for dyes, which may be π conjugated structure.

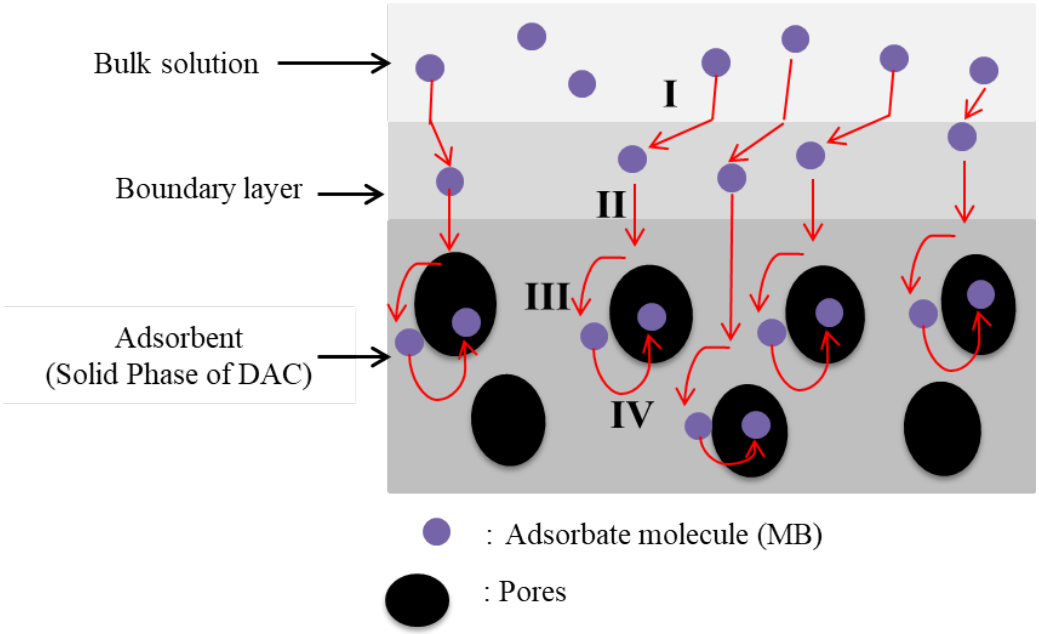

(a)

Int. Journal of Integrated Engineering Vol. 16 No. 5 (2024) p. 489-502

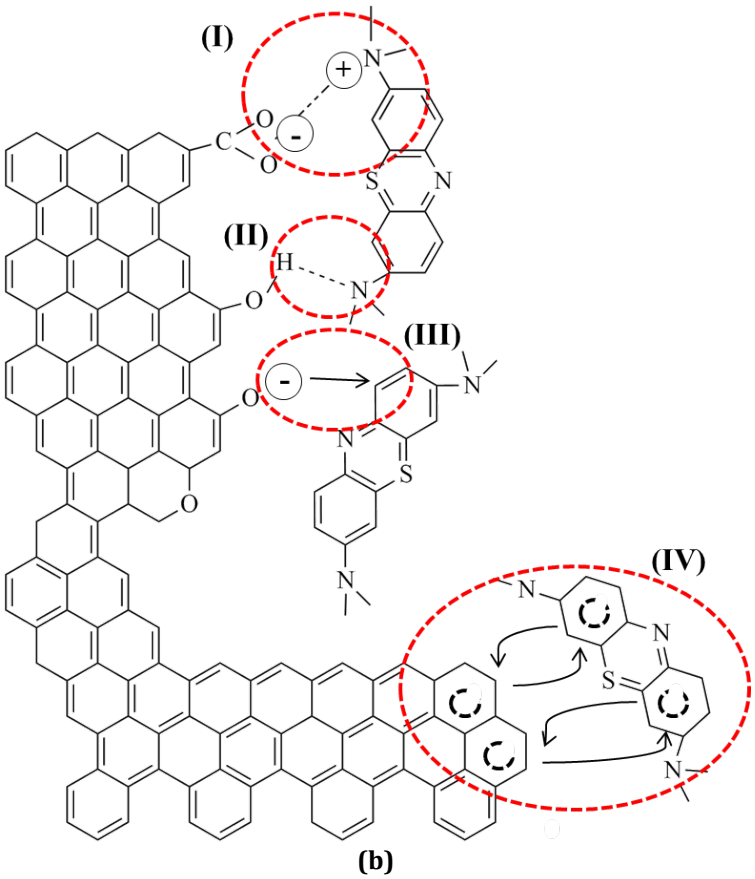

Fig. 6 *Schematic diagram of the (a) Mechanism of MB molecules adsorption by external and internal diffusion; and (b) Mechanism of interaction between DAC and AC system*

5. Conclusion

AC prepared from DS was successfully produced via chemical activation method utilising H_2SO_4 as the activating agent. On the basis of characterisation, the utilisation of H_2SO_4 as an activating agent resulted in DAC with a porous structure and a high BET surface area value (242.03 m^2/g) and total pore volume (0.028 cm^3/g). The produced DAC also presented maximum dye removal percentage and q_e of 92.05% and 0.767 mg/g, respectively. The optimum DAC dosage was 0.6 g with an optimum contact time of 15 min and 10 ppm of initial MB dye concentration.

Acknowledgement

The authors acknowledge the financial support from the Fundamental Research Grand Scheme (grant no. 2020-0254-103-02) and nternational grant Kementerian Agama Republik Indonesia (grant no. 2023-0029-103-11).

Conflict of Interest

The authors declared that they have no conflict of interest.

Author Contribution

The authors confirm contribution to the paper as follows: ***Conceptualization and supervision****: Suriani Abu Bakar; Methodology: Suriani Abu Bakar and Muqoyyanah;* ***Formal analysis and investigation****: Rosmanisah Mohamat; Resources: Suriani Abu Bakar and Azmi Mohamed;* ***Writing – Original draft****: Rosmanisah Mohamat;* ***Writing – Review & editing****: Suriani Abu Bakar, Azmi Mohamed, Azlan Kamari, Muqoyyanah, Mohd Hafiz Dzarfan Othman, Mohamad Hafiz Mamat, Mohd Khairul Ahmad, Muhammad Noorazlan, Norhayati Hashim, Mohd Ambri Mohamed, Muhammad Danang Birowosuto, Tetsuo Soga, Hamdan Hadi Kusuma, Budi Astuti, and Khuram Ali;* ***Project administration****: Suriani Abu Bakar and Azmi Mohamed;* ***Funding acquisition****: Suriani Abu Bakar and Azmi Mohamed. All authors reviewed the results and approved the final version of the manuscript.*

References

[1] Adar, E. (2020) Optimization of triple dye mixture removal by oxidation with Fenton, *International Journal of Environmental Science and Technology*, *17(11)*, 4431–4440, https://doi.org/10.1007/s13762-020-02782-1

[2] Cheng, S., Zhang, L., Ma, A., Xia, H., Peng, J., Li, C., & Shu, J. (2018) Comparison of activated carbon and iron/cerium modified activated carbon to remove methylene blue from wastewater, *Journal of Environmental Sciences*, *65*, 92–102, https://doi.org/10.1016/j.jes.2016.12.027

[3] Peydayesh, M., Mohammadi, T., & Bakhtiari, O. (2018) Effective treatment of dye wastewater via positively charged TETA-MWCNT/PES hybrid nanofiltration membranes, *Separation and Purification Technology*, *194*, 488–502, https://doi.org/10.1016/j.seppur.2017.11.070

[4] Topare, N. S., & Bokil, S. A. (2021) Adsorption of textile industry effluent in a fixed bed column using activated carbon prepared from agro-waste materials, *Materials Today: Proceedings*, *43*, 530–534, https://doi.org/10.1016/j.matpr.2020.12.029

[5] Ukkakimapan, P., Sattayarut, V., Wanchaem, T., Yordsri, V., Phonyiem, M., Ichikawa, S., Obata, M., Fujishige, M., Takeuchi, K., Wongwiriyapan, W., & Endo, M. (2020), Preparation of activated carbon via acidic dehydration of durian husk for supercapacitor applications. *Diamond and Related Materials*, *107*, 107906, https://doi.org/10.1016/j.diamond.2020.107906

[6] Marrakchi, F., Ahmed, M. J., Khanday, W. A., Asif, M., & Hameed, B. H. (2017) Mesoporous-activated carbon prepared from chitosan flakes via single-step sodium hydroxide activation for the adsorption of methylene blue, *International Journal of Biological Macromolecules*, *98*, 233–239, https://doi.org/10.1016/j.ijbiomac.2017.01.119

[7] Amin, P. D., Bhanushali, V., & Joshi, S. (2018) Role of Polyvinlyppyrrolidone in Membrane Technologies, *International Journal of ChemTech Research*, *11(9)*, 247–259, https://doi.org/10.20902/ijctr.2018.110932

[8] Igbinigun, E., Fennell, Y., Malaisamy, R., Jones, K. L., & Morris, V. (2016) Graphene oxide functionalized polyethersulfone membrane to reduce organic fouling, *Journal of Membrane Science*, *514*, 518–526, https://doi.org/10.1016/j.memsci.2016.05.024

[9] Mohamat, R., Suriani, A. B., Mohamed, A., Muqoyyanah, Othman, M. H. D., Rohani, R., Mamat, M. H., Ahmad, M. K., Azlan, M. N., Mohamed, M. A., Birowosuto, M. D., & Soga, T. (2021) Effect of Surfactants' Tail Number on the PVDF/GO/TiO_2-Based Nanofiltration Membrane for Dye Rejection and Antifouling Performance Improvement, *International Journal of Environmental Research*, *15(1)*, 149–161, https://doi.org/10.1007/s41742-020-00299-6

[10] Suriani, A. B., Muqoyyanah, Mohamed, A., Othman, M. H. D., Rohani, R., Yusoff, I. I., Mamat, M. H., Hashim, N., Azlan, M. N., Ahmad, M. K., Marwoto, P., Suhaldi, Kusuma, H. H., Birowosuto, M. D., & Abdul Khalil, H. P. S. (2019) Incorporation of electrochemically exfoliated graphene oxide and TiO_2 into polyvinylidene fluoride-based nanofiltration membrane for dye rejection, *Water Air Soil Pollution*, *230*, 176, https://doi.org/10.1007/s11270-019-4222-x

[11] Amornpitoksuk, P., Suwanboon, S., Sirimahachai, U., Randorn, C., & Yaemsunthorn, K. (2016) Photocatalytic degradation of methylene blue by C3N4/ZnO: The effect of the melamine/ZnO ratios, *Bulletin of Materials Science*, *39(6)*, 1507–1513, https://doi.org/10.1007/s12034-016-1294-8

[12] Liu, J., Wang, L., Tang, J., & Ma, J. (2016) Photocatalytic degradation of commercially sourced naphthenic acids by TiO_2-graphene composite nanomaterial, *Chemosphere*, *149*, 328–335, https://doi.org/10.1016/j.chemosphere.2016.01.074

[13] Narvekar, A. A., Fernandes, J. B., & Tilve, S. G. (2018) Adsorption behavior of methylene blue on glycerol based carbon materials, *Journal of Environmental Chemical Engineering*, *6(2)*, 1714–1725, https://doi.org/10.1016/j.jece.2018.02.016

[14] Novais, R. M., Caetano, A. P. F., Seabra, M. P., Labrincha, J. A., & Pullar, R. C. (2018) Extremely fast and efficient methylene blue adsorption using eco-friendly cork and paper waste-based activated carbon adsorbents, *Journal of Cleaner Production*, *197(Part 1)*, 1137–1147, https://doi.org/10.1016/j.jclepro.2018.06.278

[15] Taman, R., Ossman, M., Mansour, M., & Farag, H. (2015) Metal oxide nano-particles as an adsorbent for removal of heavy metals, *Journal of Advanced Chemical Engineering*, *5(3)*, 1–8, https://doi.org/10.4172/2090-4568.1000125

[16] Gurung, M., Adhikari, B. B., Kawakita, H., Ohto, K., Inoue, K., & Alam, S. (2013) Recovery of gold and silver from spent mobile phones by means of acidothiourea leaching followed by adsorption using biosorbent prepared from persimmon tannin, *Hydrometallurgy*, *133*, 84–93, https://doi.org/10.1016/j.hydromet.2012.12.003

[17] Mateen, F., Javed, I., Rafique, U., Tabassum, N., Sarfraz, M., Safi, S. Z., Yusoff, I., & Ashraf, M. A. (2016) New method for the adsorption of organic pollutants using natural zeolite incinerator ash (ZIA) and its

application as an environmentally friendly and cost-effective adsorbent, *Desalination and Water Treatment*, *57(14)*, 6230–6238. https://doi.org/10.1080/19443994.2015.1005146
[18] Dong, L., Pan, S., Liu, J., Wang, Z., Hou, L., & Chen, G. (2020) Performance and mechanism of Pb(II) removal from water by the spent biological activated carbon (SBAC) with different using-time, *Journal of Water Process Engineering*, *36*, 101255, https://doi.org/10.1016/j.jwpe.2020.101255
[19] Rashid, J., Tehreem, F., Rehman, A., & Kumar, R. (2019) Synthesis using natural functionalization of activated carbon from pumpkin peels for decolourization of aqueous methylene blue, *Science of the Total Environment*, *671*, 369–376, https://doi.org/10.1016/j.scitotenv.2019.03.363
[20] Solgi, M., Najib, T., Ahmadnejad, S., & Nasernejad, B. (2017) Synthesis and characterization of novel activated carbon from medlar seed for chromium removal: Experimental analysis and modeling with artificial neural network and support vector regression. *Resource-Efficient Technologies*, *3(3)*, 236–248, https://doi.org/10.1016/j.reffit.2017.08.003
[21] Rafatullah, M., Sulaiman, O., Hashim, R., & Ahmad, A. (2010) Adsorption of methylene blue on low-cost adsorbents : A review, *Journal of Hazardous Materials*, *177(1-3)*, 70–80, https://doi.org/10.1016/j.jhazmat.2009.12.047
[22] Geçgel, Ü., Özcan, G., & Gürpınar, G. Ç. (2013) Removal of methylene blue from aqueous solution by activated carbon prepared from pea shells (Pisum sativum), *Journal of Chemistry*, *2013(1)*, 1–9. https://doi.org/10.1155/2013/614083
[23] Nicholas, A. F., Hussein, M. Z., Zainal, Z., & Khadiran, T. (2018) Palm kernel shell activated carbon as an inorganic framework for shape-stabilized phase change material, *Nanomaterials*, *8(9)*, 689–700, https://doi.org/10.3390/nano8090689
[24] Misran, E., Bani, O., Situmeang, E., & Purba, A. (2018) Removal efficiency of methylene blue using activated carbon from waste banana stem : Study on pH influence, *IOP Conference Series:Earth and Enviromental Science*, *122*, 1–6, https://doi.org//10.1088/1755-1315/122/1/012085
[25] Sahira, J., Mandira, A., Prasad, P. B., & Ram, P. R. (2013) Effects of activating agents on the activated carbons prepared from lapsi seed stone, *Research Journal of Chemical Science*, *3*(5), 19–24.
[26] Musa, A., Alwi, S. R. W., Ngadi, N., & Abbaszadeh, S. (2017) Effect of activating agents on the adsorption of ammoniacal nitrogen using activated carbon papaya peel, *Chemical Engineering Transactions*, *56*, 841–846, https://doi.org/10.3303/CET1756141
[27] Pathania, D., Sharma, S., & Singh, P. (2013) Removal of methylene blue by adsorption onto activated carbon developed from ficus carica bast, *Arabian Journal of Chemistry*, *10*, S1445–S1451, https://doi.org/10.1016/j.arabjc.2013.04.021
[28] Tham, Y. J., Latif, P. A., Abdullah, A. M., & Taufiq-Yap, Y. H. (2010) Physical characteristics of activated carbon derived from durian shell, *Asian Journal of Chemistry*, *22(1)*, 772–780.
[29] Mahmood, W. N. W., Samsuddin, R., & Deris, R. R. R. (2015). Chemical activation of durian shell activated carbon: Effects of activation agents, *Advanced Materials Research*, *1113*, 242–247, https://doi.org/10.4028/www.scientific.net/amr.1113.242
[30] Yazidi, A., Atrous, M., Edi Soetaredjo, F., Sellaoui, L., Ismadji, S., Erto, A., Bonilla-Petriciolet, A., Luiz Dotto, G., & Ben Lamine, A. (2020) Adsorption of amoxicillin and tetracycline on activated carbon prepared from durian shell in single and binary systems: Experimental study and modeling analysis, *Chemical Engineering Journal*, *379*, https://doi.org/10.1016/j.cej.2019.122320
[31] Lee, M. C., Koay, S. C., Chan, M. Y., Pang, M. M., Chou, P. M., & Tsai, K. Y. (2018) Preparation and characterization of durian husk fiber filled polylactic acid biocomposites, *MATEC Web of Conferences*, *152*, 1–7, https://doi.org/10.1051/matecconf/201815202007
[32] Zhang, X., Cheng, L., Wu, X., Tang, Y., & Wu, Y. (2015) Activated carbon coated palygorskite as adsorbent by activation and its adsorption for methylene blue, *Journal of Enviromental Sciences*, *33*, 97–105, https://doi.org/10.1016/j.jes.2015.01.014
[33] Jawad, A. H., Razuan, R., Appaturi, J. N., & Wilson, L. D. (2019) Adsorption and mechanism study for methylene blue dye removal with carbonized watermelon (Citrullus lanatus) rind prepared via one-step liquid phase H_2SO_4 activation, *Surfaces and Interfaces*, *16*, 76–84, https://doi.org/10.1016/j.surfin.2019.04.012
[34] Srinivasakannan, C., & Bakar, M. Z. A. (2004) Production of activated carbon from rubber wood sawdust, *Biomass and Bioenergy*, *27(1)*, 89–96, https://doi.org/10.1016/j.biombioe.2003.11.002
[35] Ismail, A., Sudrajat, H., & Jumbianti, D. (2010) Activated carbon from durian seed by H_3PO_4 activation: Preparation and pore structure characterization, *Indonesian Journal of Chemistry*, *10*(1), 36–40, https://doi.org/10.22146/ijc.21495
[36] Foo, K. Y., & Hameed, B. H. (2012) Textural porosity, surface chemistry and adsorptive properties of durian shell derived activated carbon prepared by microwave assisted NaOH activation, *Chemical Engineering Journal*, *187*, 53–62, https://doi.org/10.1016/j.cej.2012.01.079

[37] Chandra, T. C., Mirna, M. M., Sunarso, J., Sudaryanto, Y., & Ismadji, S. (2009) Activated carbon from durian shell: Preparation and characterization, *Journal of the Taiwan Institute of Chemical Engineers*, *40(4)*, 457–462, https://doi.org/10.1016/j.jtice.2008.10.002
[38] Zawawi, N. M., Hamzah, F., Sarif, M., Fairuz, S., Manaf, A., & Idris, A. (2017) Characterization of activated carbon using chemical activation via microwave ultrasonic system, *Malaysian Journal of Analytical Sciences*, *21*(1), 159–165, https://doi.org/10.17576/mjas-2017-2101-18
[39] Örkün, Y., Karatepe, N., & Yavuz, R. (2012) Influence of temperature and impregnation ratio of H_3PO_4 on the production of activated carbon from hazelnut shell, *Acta Physica Polonica A*, *121*(1), 277–280, https://doi.org/10.12693/APhysPolA.121.277
[40] Baek, J., Shin, H. S., Chung, D. C., & Kim, B. J. (2017) Studies on the correlation between nanostructure and pore development of polymeric precursor-based activated hard carbons: II. Transmission electron microscopy and Raman spectroscopy studies, *Journal of Industrial and Engineering Chemistry*, *54*, 324–331, https://doi.org/10.1016/j.jiec.2017.06.007
[41] Benaddi, H., Bandosz, T. J., Jagiello, J., Schwarz, J. A., Rouzaud, J. N., Legras, D., & Beguin, F. (2000) Surface functionality and porosity of activated carbons obtained from chemical activation of wood, *Carbon*, *38(5)*, 669–674, https://doi.org/10.1016/S0008-6223(99)00134-7
[42] Haimour, N. M., & Emeish, S. (2006) Utilization of date stones for production of activated carbon using phosphoric acid, *Waste Management*, *26(6)*, 651–660, https://doi.org/10.1016/j.wasman.2005.08.004
[43] Desta, M. B. (2013) Batch sorption experiments: Langmuir and Freundlich isotherm studies for the adsorption of textile metal ions onto teff straw (Eragrostis tef) agricultural waste, *Journal of Thermodynamics*, *2013(1)*, 1–6, https://doi.org/10.1155/2013/375830
[44] Li, Z., Jia, Z., Ni, T., & Li, S. (2017) Adsorption of methylene blue on natural cotton based flexible carbon fiber aerogels activated by novel air-limited carbonization method, *Journal of Molecular Liquids*, *242*, 747–756, https://doi.org/10.1016/j.molliq.2017.07.062
[45] Hameed, B. H., Din, A. T. M., & Ahmad, A. L. (2007) Adsorption of methylene blue onto bamboo-based activated carbon : Kinetics and equilibrium studies, *Journal of Hazardous Materials*, *141(3)*, 819–825, https://doi.org/10.1016/j.jhazmat.2006.07.049
[46] Said, A., Hakim, M. S., & Rohyami, Y. (2014). The effect of contact time and pH on methylene blue removal by volcanic ash, *Int'l Conference on Chemical, Biological, and Enviromental Sciences (ICCBES'14)*, 11–13. http://dx.doi.org/10.17758/IAAST.A0514002
[47] Pelekani, C., & Snoeyink, V. L. (2000) Competitive adsorption between atrazine and methylene blue on activated carbon : the importance of pore size distribution, *38(10)*, 1423–1436, https://doi.org/10.1016/S0008-6223(99)00261-4
[48] Kannan, N., & Sundaram, M. M. (2001) Kinetics and mechanism of removal of methylene blue by adsorption on various carbons — a comparative study, *Dyes and Pigments*, *51(1)*, 25–40, https://doi.org/10.1016/S0143-7208(01)00056-0
[49] Sulyman, M., Namiesnik, J., & Gierak, A. (2017) Low-cost Adsorbents Derived from Agricultural By-products / Wastes for Enhancing Contaminant Uptakes from Wastewater: A Review, *Polish Journal of Environmental Studies*, *26*(2), 479–510, https://doi.org/10.15244/pjoes/66769
[50] Qada, E. N. El, Allen, S. J., & Walker, G. M. (2006) Adsorption of methylene blue onto activated carbon produced from steam activated bituminous coal: A study of equilibrium adsorption isotherm, *Chemical Engineering Journal*, *124(1-3)*, 103–110, https://doi.org/10.1016/j.cej.2006.08.015
[51] Vargas, A. M. M., Cazetta, A. L., Kunita, M. H., Silva, T. L., & Almeida, V. C. (2011) Adsorption of methylene blue on activated carbon produced from flamboyant pods (Delonix regia): Study of adsorption isotherms and kinetic models, *Chemical Engineering Journal*, *168(2)*, 722–730, https://doi.org/10.1016/j.cej.2011.01.067
[52] Ahmad, M., Akanji, M. A., Usman, A. R. A., Farraj, A. S. F. Al, Tsang, Y. F., & Wabel, M. I. Al. (2020) Turning date palm waste into carbon nanodots and nano zerovalent iron composites for excellent removal of methylthioninium chloride from water, *Scientific Reports*, *10*, 16125–16140, https://doi.org/10.1038/s41598-020-73097-x
[53] Hussain, I., Li, Y., Qi, J., Li, J., & Wang, L. (2018) Nitrogen-enriched carbon sheet for Methyl blue dye adsorption, *Journal of Environmental Management*, *215*, 123–131, https://doi.org/10.1016/j.jenvman.2018.03.051